ENGINEERING TRANSACTIONS • *Engng. Trans.* • **65**, 1, 113–121, 2017
Polish Academy of Sciences • Institute of Fundamental Technological Research (IPPT PAN)
National Engineering School of Metz (ENIM) • Poznan University of Technology

Validation of a New Hyperviscoelastic Model for Deformable Polymers Used for Joints between RC Frames and Masonry Infills

Arkadiusz KWIECIEŃ[1)], Matija GAMS[2)], Theodoros ROUSAKIS[3)]
Alberto VISKOVIC[4)], Jože KORELC[5)]

[1)] *Cracow University of Technology*
Institute of Structural Mechanics
Warszawska 24, 31-155 Kraków, Poland
e-mail: akwiecie@pk.edu.pl

[2)] *Slovenian National Building and Civil Engineering (ZAG)*
Dimiceva 12, 1000 Ljubljana, Slovenia

[3)] *Democritus University of Thrace*
Department of Civil Engineering
Vas Sofias 12, 67100 Xanthi, Greece

[4)] *D'Annunzio University of Chieti-Pescara*
Engineering and Geology Department
Viale Pindaro 42, 65127 Pescara, Italy

[5)] *University of Ljubljana*
Faculty for Civil and Geodetic Engineering
Jamova 2, 1000 Ljubljana, Slovenia

In the paper, an attempt to alleviate the problem of premature damage to infills by using flexible polymers between the infill and the r.c. frame is presented. The flexibility of the polymer could serve to reduce the stress concentrations and thereby reduce damage to infills on one hand, and provide a high amount of damping and ductility on the other. Its efficiency is tested by cyclic shear tests carried out on a large-scale model. In the numerical part, the material is modelled using for the purpose developed finite element. The finite element with the new hyperviscoelastic constitutive model was coded in the AceGen/AceFEM program.

Key words: deformable polymers, hyperviscoelastic model, masonry infills.

1. Introduction

Masonry infills are commonly used in 20th century architectural heritage residential and office buildings. The infills contribute to lateral stiffness as well as resistance of such construction systems. Damage to masonry infills in r.c. frame structures during earthquakes may occur at relatively modest earthquake intensity because the stiff infills are connected rigidly to the flexible frames. A new structural bonding method using a flexible polymer PM to fill new horizontal and vertical joints between infilling masonry and frame is proposed. The flexibility of the polymer could serve to reduce the stress concentrations and thereby reduce damage to infills on one hand, and provide a high amount of damping and ductility on the other. Despite the flexibility of the polymer, the brick-to-concrete joint would be capable of transferring significant loads during in-plane and out-of-plane excitations. To test the validity of this idea, a joint made of flexible polymer was tested and numerically modelled.

2. Experimental background

In the experimental research part, the behaviour of the polymer is studied on cyclic shear tests of the joint, which simulates the highly deformable joint between masonry infill and a r.c. frame structure. The brick-to-concrete joint in real scale was tested cyclically with dynamic shear loads with various frequencies.

2.1. Flexible joint made of polymer PM

The deformable material in the brick-to-concrete joint is special polyurethane (with patented additives) – polymer PM with the following properties: Young's modulus $E = 4.5$ N/mm^2, tensile strength $f_t = 0.85$–1.95 N/mm^2, ultimate strain $\varepsilon = 50$–150% (depending on the rate of load application). This material was tested in many practical applications between structural elements [1], including dynamic [2], and shear tests [3]. It has been also studied theoretically and through numerical modeling [4]. Detailed analysis of polymer PM and flexible joints made of it can be found in [5].

2.2. Setup of the dynamic cyclic shear test

For simplification, the concrete-to-concrete joint was applied in the setup, instead of the brick-to-concrete joint. It was done to simplify the test, and ensure application of a relatively high load to polymer joint. Shear loads in the test were not big enough to damage the joint. The specimen consists of two joints

between three concrete elements. The side concrete elements are fixed, whereas the middle element, where the load is applied, is free to move vertically. There is a special system for redistribution of vertical loads to the middle element. Distances between intermediate supports of the setup (Fig. 1) were calculated to assure even relative deflection of the middle element.

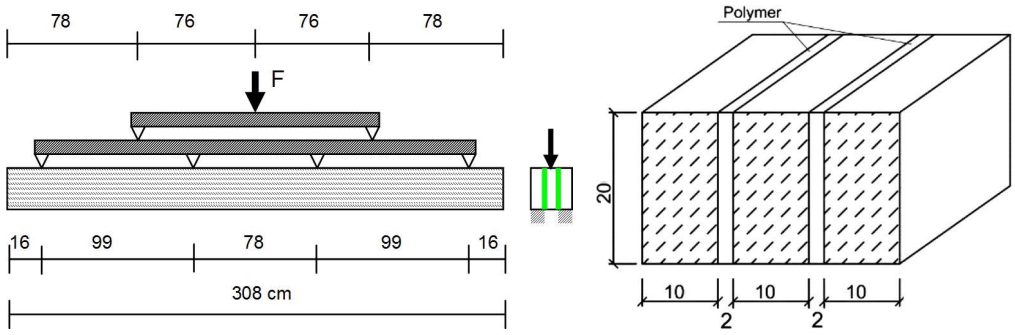

FIG. 1. Setup scheme with localization of the intermediate supports at the middle element (left) and visualization of polymer flexible joints bonding concrete elements (right).

The whole system was loaded by means of an electronically controlled hydraulic IST pulsator with displacement ratio adjusted to receive required frequencies for loading-unloading cycles. Continuous data acquisition (time, external force, deflections) was carried out with the electronic HBM devices connected to PC. The relative deflections were measured with LVDT gauges located at the middle element and the side ones at the locations of the intermediate supports. The mean value of the total relative displacement is used in graphical presentation of the results.

2.3. Cyclic shear test of the flexible joint

The cyclic shear test was carried out with two frequencies: 0.05 and 1 Hz (Fig. 2). At the beginning of each cyclic test, the initial load of 200 kN was applied.

Next 30 cycles in the load range 10–390 kN were performed on the double joint with dimensions $308 \times 20 \times 2$ cm. The obtained results in form of hysteretic loops (force-deflection) are presented in Fig. 2. They indicate that the areas of the loop are not very different for different frequencies. The calculated damping ratio for the cyclic shear tests ($D = 0.02$) is 3 times lower than the damping ratio determined in tensile-compression test [2].

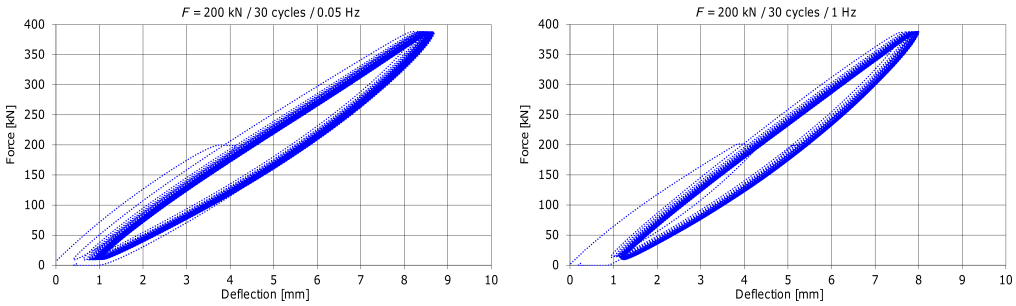

FIG. 2. Hysteretic loops force-deflection (30 cycles of shear loading), applied to the flexible joint made of polymer PM. Middle point $F = 200$ kN, loading range 10–390 kN, frequencies: 0.05 and 1 Hz.

3. Constitutive modelling and numerical analysis

3.1. New D-N strain measure

Experimental tests on the flexible polymer have shown that the material is capable of very large deformations and exhibits strongly time dependent (viscous) hyperelastic behavior which cannot be modelled accurately using Saint-Venant-Kirchhoff (SVK) material and Seth-Hill strain measures $\mathbf{E}^{(m)}$ [4, 5]. In cyclic tests, the material is capable of dissipating energy, which is clear from the area enclosed by the hysteretic loops.

Here the first attempts at modelling time dependent response of the material are presented using the special strain measures and taking into account viscous effects. The same numerical model is then used to model cyclic response, but performs poorly due to model's inability to properly include hysteretic effects and damping.

To improve the simulations using the Seth-Hill [6] strain tensors $\mathbf{E}^{(m)}$ expressed by the right stretch tensor $\mathbf{U}^m$ with index m and of the approximation of the Hencky strain tensor in form $\mathbf{E}^{(n)} = (\mathbf{U}^n - \mathbf{U}^{-n})/2n$, presented in [7] (which are not accurate enough [8–10] for the polymer PM), a new Darijani-Naghdabadi (D-N) family of strain measure $\mathbf{E}^{(\alpha,\,\beta)}$ (see Eq. (3.1)) was proposed in the Lagrangian description with a conjugate stress tensor $\mathbf{T}^{(\alpha,\,\beta)}$, shown in Eq. (3.2) – where α and β are defined in Eq. (3.1) [8, 11], and λ_1 represent principal stretches. The constitutive equation is written in principal directions not in its general form. Strain measures $\mathbf{E}^{(\alpha,\,\beta)}$ and stresses $\mathbf{T}^{(\alpha,\,\beta)}$ are objective. In the case $m = \alpha + \beta = 0$, the D-N family of strains simplifies to the Hencky model (i.e logarithmic strains). The form of strain energy remains the same as the SVK model and is shown in Eq. (3.3) with the Lame constants μ and Λ.

$$\mathbf{E}^{(\alpha+\beta)} = \frac{1}{\alpha+\beta}\left(\mathbf{U}^{\alpha} - \mathbf{U}^{-\beta}\right), \tag{3.1}$$

$$\mathbf{T}^{(\alpha,\beta)} = \frac{2\mu}{\alpha+\beta}\begin{bmatrix} \lambda_1^{\alpha}-\lambda_1^{-\beta} & & \\ & \lambda_2^{\alpha}-\lambda_2^{-\beta} & \\ & & \lambda_3^{\alpha}-\lambda_3^{-\beta} \end{bmatrix} + \frac{\Lambda}{(\alpha+\beta)}\left(\lambda_1^{\alpha}-\lambda_1^{-\beta}+\lambda_2^{\alpha}-\lambda_2^{-\beta}+\lambda_3^{\alpha}-\lambda_3^{-\beta}\right)\begin{bmatrix} 1 & & \\ & 1 & \\ & & 1 \end{bmatrix}, \tag{3.2}$$

$$W\left(\mathbf{E}^{(\alpha,\beta)}\right) = \mu tr\left(\mathbf{E}^{(\alpha,\beta)}\right)^2 + \frac{\Lambda}{2}\left(tr\mathbf{E}^{(\alpha,\beta)}\right)^2. \tag{3.3}$$

The equations presented above were implemented into a 3D finite element using AceGen [12, 13], a system for automatic generation of a finite-element code, using in many applications [14, 15]. A finite element was developed based on the D-N family of strain measures (3.1) and a classical viscosity model [16]. The model is time (rate) dependent and based on the split to volumetric and deviatoric stresses. The deviatoric stresses are calculated as presented in Eqs. (3.4) and (3.5). For details of the numerical implementation, please refer to [9]:

$$T_d = 2\mu\left((1-\nu)E_d + \nu q\right), \tag{3.4}$$

$$q = \frac{t_r}{t_r+\Delta t}E_d + \frac{t_r}{(t_r+\Delta t)(q_n - E_{d,n})}. \tag{3.5}$$

In Eqs. (3.4) and (3.5) subscripts d and n denote deviatoric part and previous time step, respectively (hence T_d, E_d and $E_{d,n}$ are deviatoric stress, deviatoric strain and deviatoric strain in previous time step), μ is the Lame constant, ν the Poisson's ratio and q an auxiliary variable (q_n is its value in previous time step), t_r is the relaxation time (material property for viscosity in this formulation).

3.2. Uniaxial tests at different load rates

Using the presented hyperviscoelastic formulation, a very good correlation between the uniaxial tensile test with monotonic loading at different rates on one hand and numerical simulations on the other, can be obtained. Comparison between experimental and numerical uniaxial tensile tests of polymer PM with various displacement rates and with Poisson's ratio assumption of $\nu = 0.49$ is shown in Fig. 3. Note that different values of α and β had to be used for different load rates to get a good match. The relaxation time t_r was 25 000 s in all numerical analyses (Table 1).

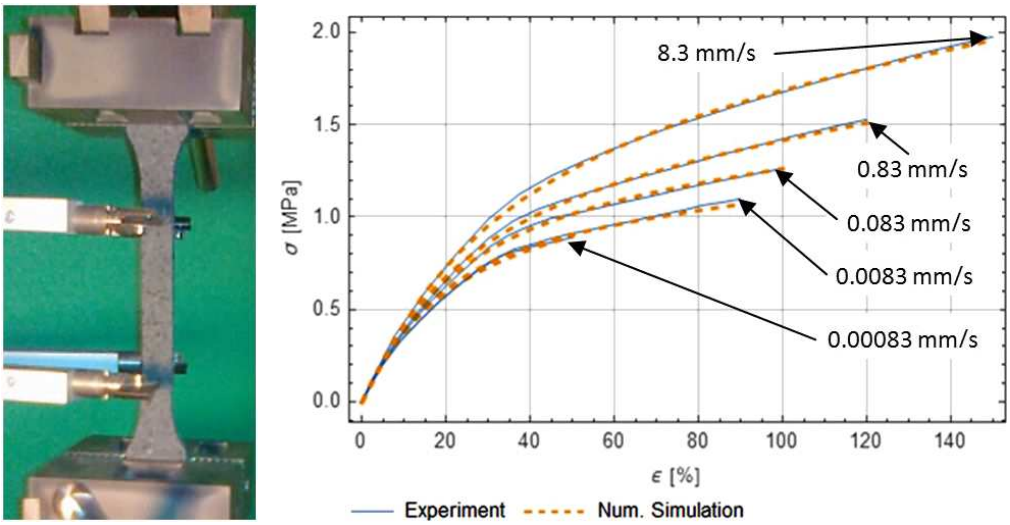

FIG. 3. Uniaxial tensile test of the polymer PM dog bone specimen (left), stress-strain curves of PM for various displacement rates (right).

Table 1. D-N model parameters for different rates of uniaxial tension of dog bone specimens.

N	1	2	3	4	5
Displacement rate [mm/s]	8.3	0.83	0.083	0.0083	0.00083
α [–]	0.8	0.87	0.85	0.97	1.0
β [–]	1.15	1.53	1.64	1.96	1.43
t_r [s]	25 000	25 000	25 000	25 000	25 000

3.3. Numerical model of cyclic shear test implemented into AceFEM

Cyclic shear tests presented in Section 2 were modelled in AceFEM, taking into account the single slice (plane strain state) and symmetry (through boundary conditions) – Fig. 4. The concrete was modelled using linear elastic finite material model ($E = 30$ GPa, $\nu = 0.2$), and the polymer is modelled using the hyperviscoelastic model with the same material properties as in Subsec. 3.2: $\alpha = 0.8$, $\beta = 1.15$ and $t_r = 25\,000$ s for the 0.05 Hz frequency, and $\alpha = 0.87$, $\beta = 1.53$ and $t_r = 25\,000$ s for the 1 Hz load frequency.

Unfortunately, the model is unable to reproduce the width (area) of the loops (see Fig. 5, where the results of the numerical simulations are drawn in red).

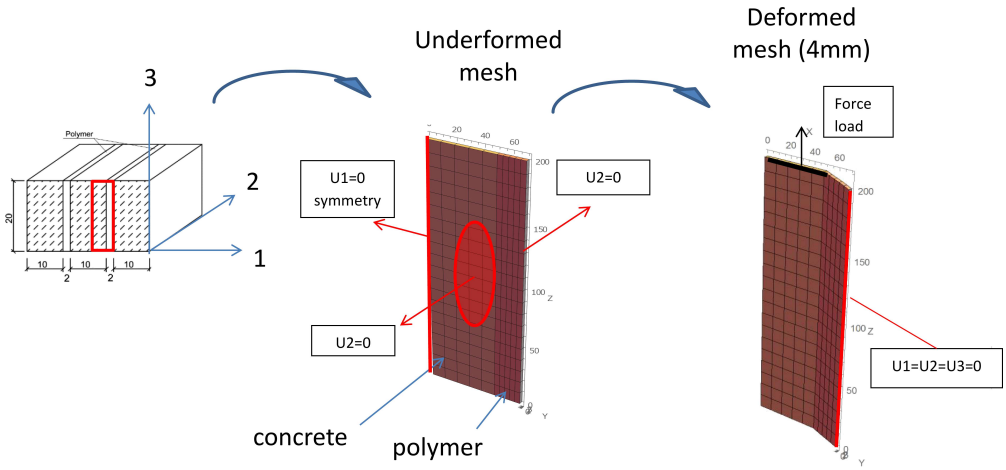

FIG. 4. Numerical model in AceFEM.

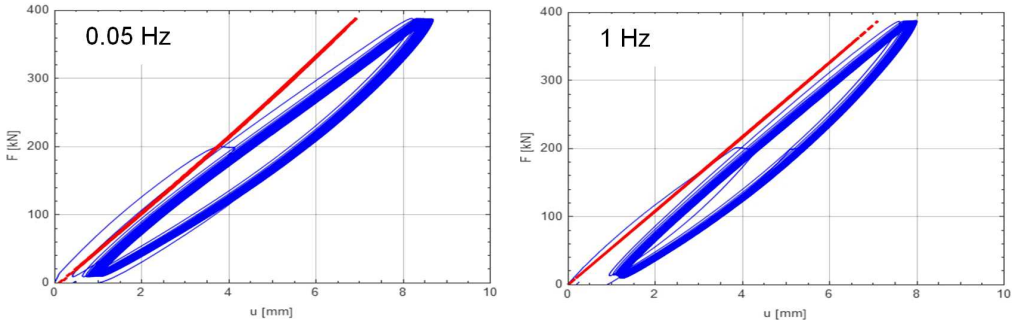

FIG. 5. Comparison of experimental force-deflection loops for frequencies: 0.05 and 1 Hz (in blue) and obtained results of the numerical simulations for the new hyperviscoelastic model (in red).

4. CONCLUSIONS

The dynamic cyclic experimental test on a polymer PM joint is presented together with the first attempts at numerical modelling of the time dependent behavior of the material model. As a first attempt a hyperviscoelastic model using a new family of strain measures is used together with viscosity. The formulation is implemented into a finite element using the AceFEM program. Numerical results are very good for monotonic tensile test at different load rates. For the cyclic shear tests, however, the results are not good, as the numerical model lack the capability of modelling hystereic effects. The formulation will be expanded in the future to improve the model's hysteretic response, and will probably include the Mullins effect [17].

References

1. Kwiecień A., *Highly deformable polymers for repair and strengthening of cracked masonry structures*, GSTF International Journal of Engineering Technology (JET), **2**(1): 182–196, 2013, doi: 10.5176/2251-3701_2.1.53.

2. Falborski T., Jankowski R., Kwiecień A., *Experimental study on polymer mass used to repair damaged structures*, Key Engineering Materials, **488–489**: 347–350, 2012, doi: 10.4028/www.scientific.net/KEM.488-489.347.

3. Kisiel P., *The stiffness and bearing capacity of polymer flexible joint under shear load*, Procedia Engineering, **108**: 496–503, 2015, doi: 10.1016/j.proeng.2015.06.111.

4. Kwiecień A., Gams M., Zając B., *Numerical modelling of flexible polymers as the adhesive for FRPs*, FRPRCS-12 & APFIS-2015 Joint Conference, p. 154, Nanjing, China, 2015.

5. Kwiecień A., *Polymer flexible joints in masonry and concrete structures* [in Polish], Monography, A Series of Civil Engineering, No. 414, Wydawnictwo Politechniki Krakowskiej, Kraków, 2012.

6. Seth B.R., *Generalized strain measure with applications to physical problems*, [in:] *Second-Order Effects in Elasticity, Plasticity, and Fluid Dynamics*, Reiner M., Abir D. [Eds.], pp. 162–171, Pergamon Press, Oxford, 1964.

7. Bažant Z.P., *Easy-to-compute tensors with symmetric inverse approximating Hencky finite strain and its rate*, Journal of Engineering Materials and Technology, Transactions of the ASME, **120**(2): 131–136, 1998, doi: 0.1115/1.2807001.

8. Darijani H., Naghdabadi R., *Constitutive modeling of solids at finite deformation using a second-order stress-strain relation*, International Journal of Engineering Science, **48**(2): 223–236, 2010, doi: 10.1016/j.ijengsci.2009.08.006.

9. Jemioło S., *Study of hyperelastic properties of isotropic materials. Modeling and numerical implementation. Scientific Works. Civil Engineering* [in Polish], Nr 140, OWPW, Warszawa, 2002.

10. Jemioło S., *Constitutive relationships of hyperelasticity* [in Polish], PAN, KILiW, Warszawa, 2016.

11. Kwiecień A., *Modeling of constitutive equations for hyperelastic polymers in flexible joints*, Modern Structural Mechanics in Engineering Design Studies in the Field of Engineering, No. 92, PAN KILiW, Garstecki A., Gilewski W., Pozorski Z. [Eds.] [in Polish], pp. 153–180, Politechnika Warszawska, Warszawa, 2015.

12. Korelc J., *Automatic generation of finite-element code by simultaneous optimization of expressions*, Theoretical Computer Science, **187**(1–2): 231–248, 1997, doi: 10.1016/S0304-3975(97)00067-4.

13. AceGen 7.0 and AceFEM 7.0 user manual, http://symech.fgg.uni-lj.si/.

14. Wcisło B., Pamin J., *Entropic thermoelasticity for large deformations and its AceGen implementation*, [in:] Łodygowski T., Rakowski J., Grabowski T. [Eds.], *Recent Advances in Computational Mechanics*, pp. 319–326, CRC Press Taylor & Francis Group, London, 2014.

15. Wcisło B., Żebro T., Kowalczyk-Gajewska K., Pamin J., *Finite strain inelastic models with gradient averaging and AceGen implementation*, Proceedings of European Congress on Computational Methods in Applied Sciences and Engineering – ECCOMASS 2012, e-Book Full Papers, pp. 5673–5687, Vienna, 2012.

16. Wriggers P., *Nonlinear finite element methods*, Springer, Berlin Heidelberg 2008.

17. Nowak Z., *Constitutive modeling and parameter identification for rubber-like materials*, Engineering Transactions, **56**(2): 117–157, 2008.

Received November 2, 2016; accepted version December 11, 2016.